

Non-uniform mesh for embroidered microstrip antennas

ISSN 1751-8725

Received on 14th October 2016

Revised 19th January 2017

Accepted on 13th February 2017

doi: 10.1049/iet-map.2016.0901

www.ietdl.org

Shiyu Zhang¹ , William Whittow¹, Rob Seager¹, Alford Chauraya¹, J(Yiannis) C. Vardaxoglou¹

¹Wolfson School Mechanical Electrical and Manufacturing Engineering, Loughborough University, Leicestershire, LE11 3TU, UK

 E-mail: S.Zhang@lboro.ac.uk

Abstract: This study presents a non-uniform meshed embroidered structure for wearable microstrip patch antennas. The non-uniform meshed patch antenna (NMPA) has significantly less conductor coverage than a conventional patch antenna without significantly compromise the antenna performance. For wearable applications, less conductor coverage reduces the usage of the specialised conductive materials which are currently expensive. The embroidered NMPA reduced manufacturing cost and improves the flexibility. In this study, the surface current distribution and the effect of the meshing size of NMPAs have been simulated and analysed. Fully textile embroidered NMPA on felt substrate has been fabricated and measured. Representative results showed the NMPA had a 60% total antenna efficiency with 20% conductor area coverage.

1 Introduction

Wearable technology has been widely studied in recent years. It has been adopted in large numbers of on-body applications including on-body networks [1], location tracking [2], fitness monitoring [3], and medical sensors [4]. Low-profile, light-weight, wireless connection and multifunctionality are required by modern wearable applications. Microstrip patch antennas can be integrated into daily garments seamlessly as they are flexible and have low profile. The ground planes of the patch antennas also shield the antennas from the human body, which means the patch antennas are less affected by the presence of a human compared with the antennas without ground planes, such as dipoles. An ideal wearable antenna should be flexible using textile materials. Embroidery is a promising technique for fabricating flexible conducting patterns [5–8].

One of the challenges of deploying embroidered patch antennas is the substantial cost of these specialist conductive textile materials. For instance the current cost of conductive thread Amberstrand Silver 66 [9] is approximately £1 per metre. Approximately 6.6 m of thread is required for the radiation element of a 2.4 GHz patch antenna [10]. Reducing the cost of manufacturing embroidered antennas will produce cost-efficient devices and encourage the development of wearable technology. Furthermore, an embroidered pattern with low stitch density is likely to have advantages of being lighter and more flexible. However, the trade-off for those advantages is reduced resonant frequency and lower antenna gain [11–14]. Therefore, an improved embroidered design that minimises the thread usage and overcomes the antenna performance reduction will benefit embroidered patch antennas.

For embroidered patch antennas, the radiation elements are composed of the embroidered stitches and the spaces between the stitches. This non-continuous surface, due to the nature of a textile, makes the conductive textiles differ from conventional conductors. Since most fabrics are normally formed by many threads on a warp and a weft, they are generally in dense meshed structures. Thus textile-based antennas are literally composed of numerous crossed lines and small meshes that are uniformly distributed.

Conventional rigid meshed patch antennas (MPAs) having orthogonal lines have been investigated for realising transparency for applications such as car windows or solar cells [15–21]. The orthogonal conductors construct uniformly distributed meshes on the MPAs which distort the surface current distribution and result in lower resonant frequency [20, 22]. However, the meshes also reduce the gain of MPAs compared with equivalent solid patch antennas [20, 23].

This paper proposes a novel non-uniform meshed structure that not only significantly reduces the conductive thread usage for embroidered microstrip patch antennas, but also minimises the antenna performance reduction. In Section 2, simulations are carried out to analyse the non-uniform meshed patch antennas (NMPAs) by investigating the resonant frequency, surface current distribution and antenna efficiency. Section 3 presents the effect of meshing the ground plane. The embroidered patch antenna was firstly examined on a laminated substrate in Section 4 to compare the embroidered NMPA with copper equivalent NMPA. Later textile material, felt, is used for the substrate in Section 5 to realise a flexible textile-based embroidered NMPA and promising measured results are presented. The final conclusions are made in Section 6.

2 Non-uniform meshed microstrip antenna

An MPA with a uniform meshing is shown in Fig. 1a. The current distribution on such an MPA for the TM_{01} mode is similar to a rectangular solid patch for the same mode, i.e. it is mainly dominated by vertically directed current. Therefore, the NMPA is designed based on this concept: to reduce the number of horizontal conductor paths that are less important for the TM_{01} mode. The NMPA is shown in Fig. 1b. The number of vertical lines is the same as for the MPA in Fig. 1a. However, there are only three horizontal lines: two along the top, bottom, and at the feed point creating a path to allow current flow from the feed point into the vertical lines. The reduced number of horizontal lines means the NMPA requires less conductive material than the MPA.

The MPAs generally have lower resonant frequency than solid patch antennas with the same exterior dimensions because the distorted surface currents result in longer electrical lengths. However, since the NMPA has fewer horizontal lines, there are less current paths available in the horizontal direction (see Fig. 1). It follows that the distortion of the current on the NMPA is less significant when compared with the MPA. Consequently, the electrical length of the NMPA is shorter than the MPA and the resonant frequency of the NMPA is higher than the MPA (for the same horizontal mesh space). A set of simulations were carried out to analyse the effect of the mesh spacing, d_W . IMST EMPIRE XCcel (finite difference time domain method) was used to simulate the antennas. The dimensions of the MPA and NMPA were $W = 37$ mm and $L = 28$ mm. They were placed on $90 \text{ mm} \times 70 \text{ mm} \times 1.57$ mm substrates (dielectric constant = 4.5 and loss tangent = 0.0037). The feed point is shown as the white spot in Fig. 1. Simulations

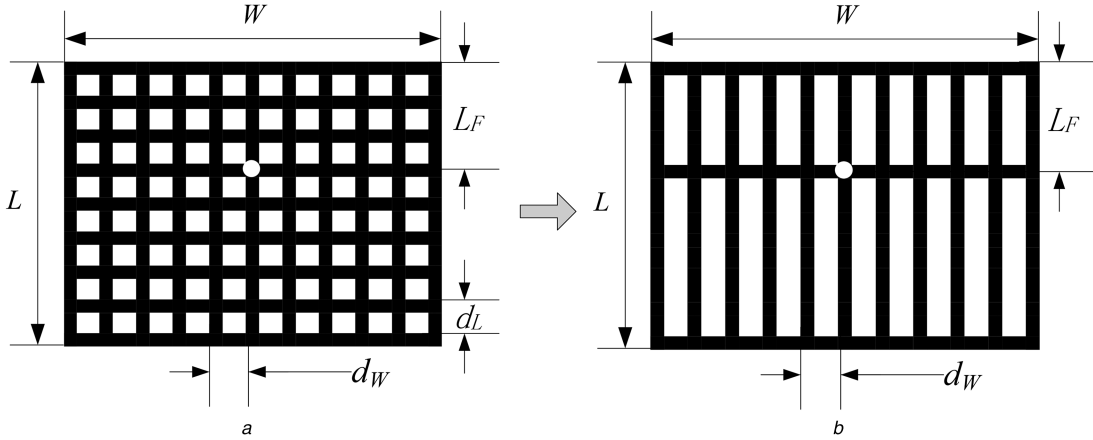


Fig. 1 Comparison between uniform meshed and non-uniform meshed patch structures

(a) Uniform meshed patch structures, (b) Proposed new non-uniform meshed patch structures

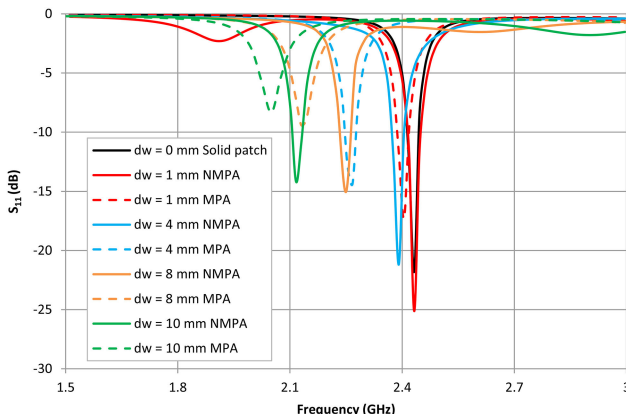


Fig. 2 Simulated S_{11} of NMPAs and MPAs with different mesh spaces d_W

were used of find the optimal feed point L_F . All the mesh line widths were 0.2 mm, equivalent to an embroidered conductive thread stitch. All the MPAs have $d_L = d_W$. Note, the distances between the two outermost vertical lines were smaller than the d_W in order to maintain the exterior dimensions.

Fig. 2 shows the simulated the S_{11} results with $d_W = 1$ mm, 4 mm, 8 mm and 10 mm, respectively. The simulated results demonstrate that larger d_W results in lower resonant frequencies. On the other hand, all the NMPAs (solid line) have higher resonant frequencies than the MPAs (dashed line) with the same mesh space d_W . A solid patch antenna with the same exterior dimension on the same substrate was simulated for comparison. It can be seen that the NMPA with 1 mm mesh space has approximately the same resonant frequency as the solid patch, which indicates that the frequency reduction is negligible for a tight meshing.

The surface current on the NMPA at its fundamental frequency is shown in Fig. 3a. It can be observed that the middle horizontal line directs the current from the feed point to both left and right sides of the NMPA, and the current flows into the vertical lines at the junctions with the horizontal lines. The largest current still flows in the vertical direction. It can be seen from Fig. 3a that higher current values appear not only on the two side edges of the NMPA, but also on the three horizontal lines. This indicates that the top and bottom frames of the NMPA are important as the middle horizontal line for guiding the current. Fig. 3b shows the simulated electric field of the NMPA which shows that the strong electric fields on the radiation edges are similar to a solid patch antenna at the TM_{01} mode. Therefore, the reduced horizontal conductor paths of the NMPA do not change the antenna radiation mode.

The simulated antenna gains and efficiencies of the NMPAs with different d_W are shown in Table 1. The gain values are taken at their resonant frequencies and include the mismatch loss. The conductor coverage percentage is the ratio of the area that is

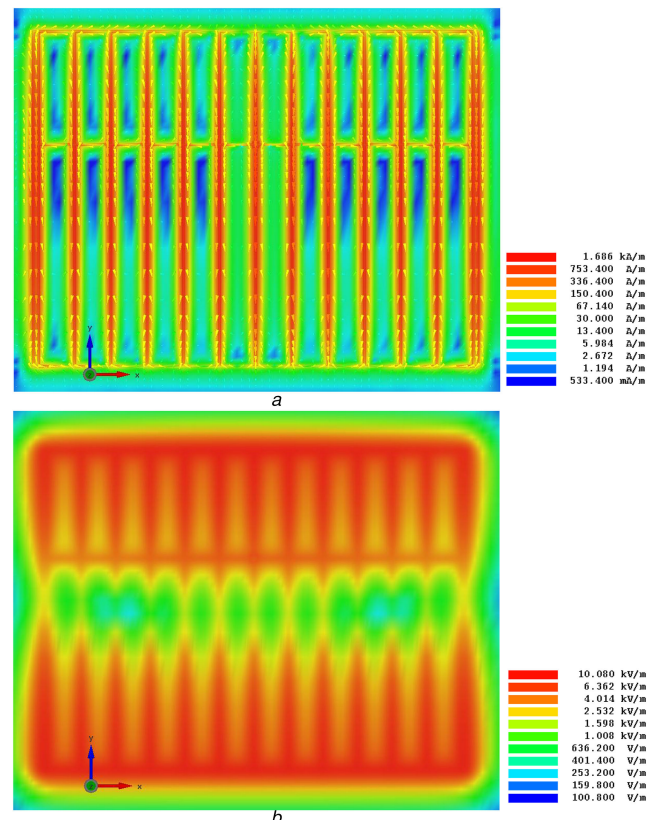


Fig. 3 Simulations of surface current distribution and electric fields of NMPA over solid substrates and ground planes

(a) Surface current distribution of NMPA, (b) Electric fields of NMPA

covered by conductive material compared to a solid patch ($37 \text{ mm} \times 28 \text{ mm}$). This ratio indicates the usage of material and a smaller value means lower material cost. It is clear that the conductor coverage is reduced significantly with larger meshing. For instance, the solid patch surface area is 1036 mm^2 and the conductor coverage can be reduced to 235.92 mm^2 if a 1 mm spacing non-uniform meshing is employed. Although the antenna gain and efficiency are reduced due to the increased mesh spacing, the 1 mm meshed NMPA still has a reasonable antenna performance (5.7 dBi gain and 68.1% total efficiency) with only 22.7% conductor coverage. The reduced efficiency is due to both conductor loss and dielectric loss. Simulations indicated that the 1 mm NMPA efficiency could be improved to 82% if the substrate was lossless and it could be further increased to 99% if the meshing was perfect electric conductor (PEC) with a lossless substrate. Fig. 4 shows the simulated total antenna efficiencies of both NMPAs and MPAs as a function of the conductor coverage. It clearly shows that for the same conductor coverage, the NMPA has a higher efficiency than

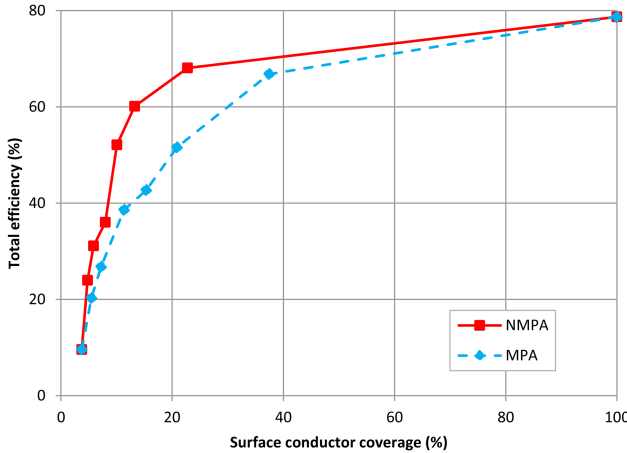


Fig. 4 Simulated total efficiency as a function of conductor surface coverage

Table 1 Simulation results of non-uniform meshed patch antennas

Mesh spacing in vertical direction, mm	Solid infill patch	1 mm NMPA	4 mm NMPA	8 mm NMPA	10 mm NMPA
conductor area, mm ²	1036	235.92	82.48	60.56	49.60
conductor coverage, %	100	22.77	7.96	5.85	4.79
gain, dBi	6.3	5.7	2.8	2.2	0.9
directivity, dBi	7.3	7.4	7.3	7.2	7.1
total efficiency, %	80.0	68.1	36.0	31.1	24.0

the MPA. Therefore, the fabric-based embroidered patch antennas should employ the non-uniform meshing, not only because of reduced material cost but also improved antenna performance.

3 Meshed ground plane

For a conventional microstrip patch antenna, there is more conducting material on the ground plane than in the radiating element. Meshing the ground plane can potentially reduce the conductive fabric usage significantly. However, a meshed ground plane causes backwards radiation, which makes the patch antenna bidirectional and results in energy absorbed by the body. Fig. 5 shows the simulated antenna gain patterns of rectangular solid patch antennas with meshed ground planes. All the patch antennas have the same exterior dimensions as in Section 2. Fig. 5 shows that the antenna gain is reduced by the increased meshing size on the ground, although all the patch antennas have solid radiation elements. Furthermore, the back-lobe is significantly increased by larger meshes, which decreases the front-to-back ratio. A patch antenna with a solid ground has a 15.3 dB front-to-back ratio, which decreases to 12.4 dB when 1 mm uniform meshing is applied on the ground plane. It is further reduced to 4.83 dB with a 4 mm meshed ground plane.

Further simulations were carried out to place these patch antennas with meshed ground planes 2 mm away from a cuboid (140 mm × 120 mm × 20 mm) phantom ($\epsilon_r = 35.4$ and conductivity = 1.8 S/m at 2.4 GHz [24]). The simulated results indicated that a patch antenna with solid ground plane had 79% radiation efficiency with the present of cuboid phantom. However, the radiation efficiency of the patch antenna with 1, 2 and 4 mm meshed ground planes were reduced to 61, 42 and 21%, respectively.

A wearable antenna is strongly affected by the detuning and dielectric loading due to the presence of the human body. A low front-to-back ratio wearable patch antenna would result in more power being radiated towards the human body. This would result in a heavily degraded antenna performance including impedance matching and antenna efficiency. A solid ground plane in wearable patch antennas can reduce the backwards radiation. A flexible ground plane that is fabricated using a flexible conductive fabric sheet (non-meshed) such as Nora-Dell [25] or Taffeta [26] is a solution that can be used for embroidered patch antennas. Digital

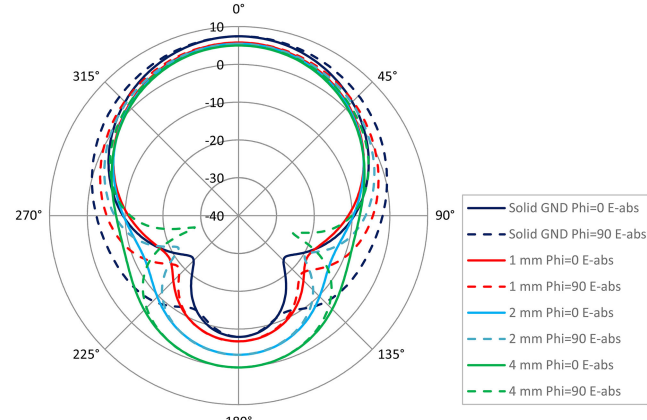


Fig. 5 Simulated radiation pattern (in dBi) of patch antennas with meshed ground planes

embroidery is used for fabricating precise and aesthetic patterns for patch antennas. This can also potentially save manufacturing time.

4 Embroidered non-uniform meshed microstrip antenna on rigid substrate

A digital embroidery machine (model: Brother Entrepreneur® Pro PR1000e) was used for fabricating the embroidered NMPA. Multi-thread conductive yarn Amberstrand Silver 66 was used. One single thread of Amberstrand Silver 66 is composed of 66 *identical* filaments. The diameter of each filament is approximately 17 μm (see Fig. 6a). Every single filament is a silver coated Zylon® fibre (a synthetic polymer material). A DC resistance measurement was taken and showed that the resistance of one Amberstrand Silver 66 thread was 2 Ω per foot which agreed with its datasheet. Scanning electron microscope (SEM) images of the Amberstrand Silver thread were taken at Loughborough University and indicated that the silver cladding layer for each filament fibre was approximately 1 μm (see Fig. 6b).

Initially, the embroidered NMPA was examined on a rigid substrate and compared with an equivalent etched NMPA. This excluded all the variables such as substrate thickness of textiles and investigated the embroidered NMPA only. The embroidered NMPA was affixed on the Taconic RF-45 substrate ($\epsilon_r = 4.5$ and $\tan\delta = 0.0037$). The embroidered 1 mm spacing NMPA (37 mm × 28 mm) on a denim fabric is shown in Fig. 7a. The three horizontal lines were embroidered three times at the same positions, respectively, for better current guiding. The embroidered stitch length was 2 mm to fit with the adjusted thread tension that was suitable for the Amberstrand Silver 66 thread. Overtightened thread would cause wrinkled fabric and a distorted pattern. The thread can also be broken frequently if the tension was too high. On the other hand, lower tension or over long stitches would result in loops on top of the embroidery due to the poor thread control. Too short stitch length not only led to a longer fabrication time but also to more thread usage.

Since the conductive threads were embroidered only on one side of the base fabric, the embroidered patch was placed upside down (see Figs. 7b and c) to eliminate the denim as an additional substrate between the radiation element and the substrate. A small copper feed pad (2 mm × 2 mm, see Fig. 7c) was etched on the substrate to increase the contacting area between the feed and the

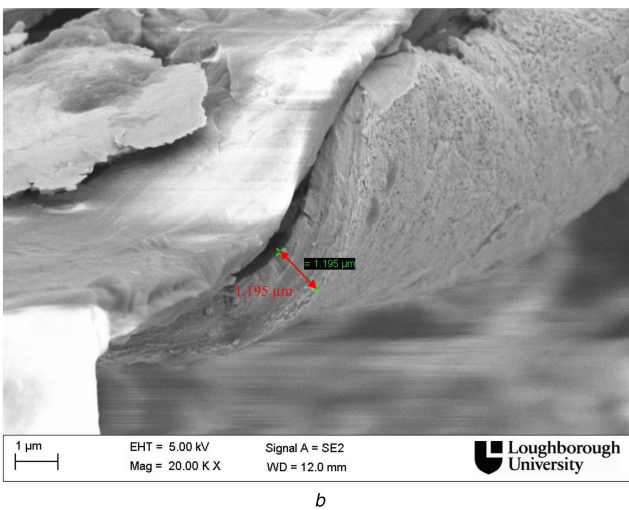
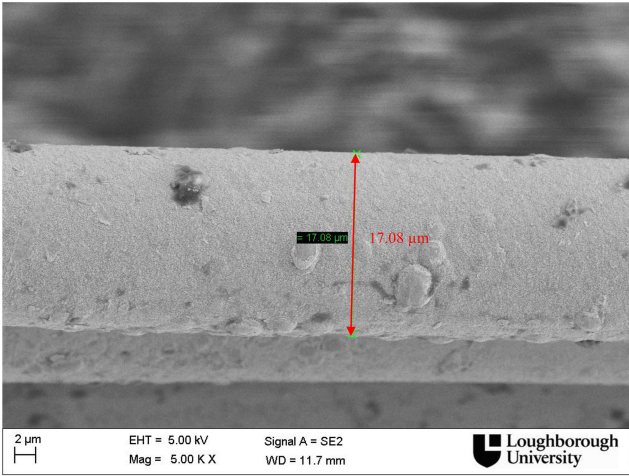


Fig. 6 SEM images of

(a) Single filament of Amberstrand Silver thread and (b) SEM image of broken section of coated layer

embroidered Amberstrand thread for better connection. The feed pad was soldered to the inner pin of the feed coaxial cable. The solder spot was then pared down to minimise its thickness. Thermal melt copolyamide adhesive web was used for affix the embroidered NMPA onto the substrate. A hole was cut at the centre of the thermal melt adhesive to avoid isolating the feeding from the embroidered NMPA. This feeding method has been proven to have good reliability [10]. The thickness of the thermal adhesive was negligible after melting. The denim fabric was approximately 0.5 mm thick and had $\epsilon_r = 1.97$, $\tan\delta = 0.074$ as measured using a split post dielectric resonator (SPDR) [27]. Simulations indicated that the very thin denim layer on top of the NMPA had negligible effects on the resonant frequency and antenna efficiency.

The measured antenna S_{11} performance is shown in Fig. 8a. The etched copper NMPA with the same specification (i.e. dimensions, mesh spacing) is included as a comparison. As shown in Fig. 8a, the resonant frequency of the embroidered patch antenna is 60 MHz lower than the equivalent etched copper patch. This is because the actual length of the embroidered stitch is longer than its dimension as a straight line, which results in a slightly longer electrical length. The actual thread length on the L edge of the embroidered NMPA is approximately 28.9 mm which is 3% longer than the pattern length L . The measured results of the etched copper NMPA all agreed well with the simulation. The measured radiation patterns of the embroidered 1 NMPA are shown in Fig. 8b. The embroidered 1 mm NMPA antenna has 3.5 dBi gain and 39% total efficiency, which includes the mismatch loss, whilst the etched NMPA copper patch has 6.0 dBi gain with 68% total efficiency. The reduced antenna gain and efficiency of the embroidered NMPA are mainly due to the thin cladding layer

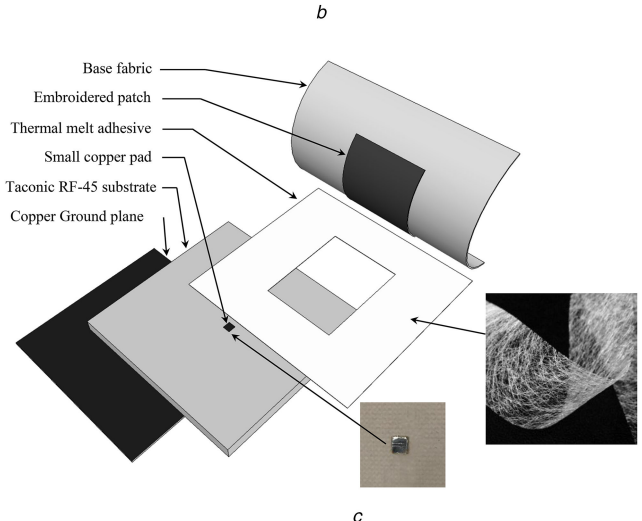
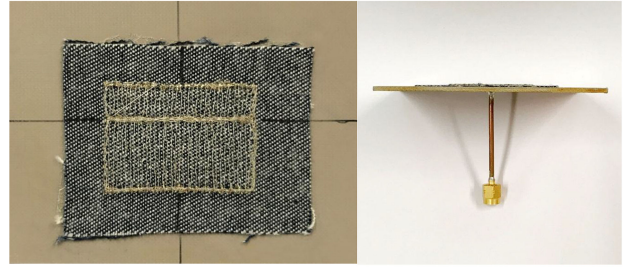
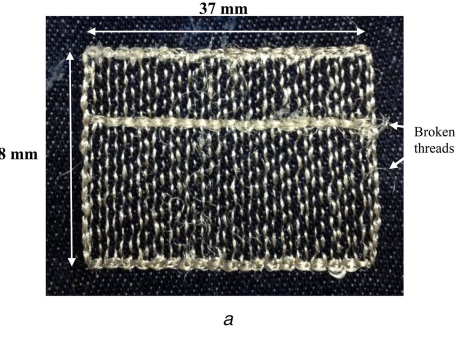


Fig. 7 (a) Embroidered 1 mm spaced NMPA before being placed on substrate, (b) Embroidered patch was affixed upside down on Taconic RF-45 substrate, with a RG-405 semi-flexible coaxial cable feeding, (c) Sketch of upside down embroidered patch antenna on rigid dielectric substrate, with thermal melt adhesive between base fabric and substrate

thickness of the Amberstrand thread. As shown in Fig. 6b, the silver coating is approximately 1 μm, which is thinner than one skin depth of silver (1.3 μm at 2.4 GHz). As a result, the skin effect increased ohmic loss and reduced the antenna efficiency. Simulations indicate that using PEC for the NMPA can improve total efficiency of the 1 mm NMPA on the Taconic RF45 substrate from 68 to 81%. In addition, several filaments of the thread were broken during the embroidery due to the friction between the thread and the needle. The breakages (see Fig. 7a) of the filaments result in higher resistance of the thread which increases the conductor loss.

5 Fully textile embroidered non-uniform patch antenna

The rigid laminate substrates were previously used to understand the effect of non-uniform meshing but they were not fully flexible as would be expected for textiles. Compared with the conventional laminate substrates, textile fabrics generally have lower permittivity and lower loss due to the microscopic air voids. The air voids also make the textile substrate light-weight and breathable which benefits antennas for wearable applications. A felt fabric and Nora-Dell were used as the flexible substrate in this work. The

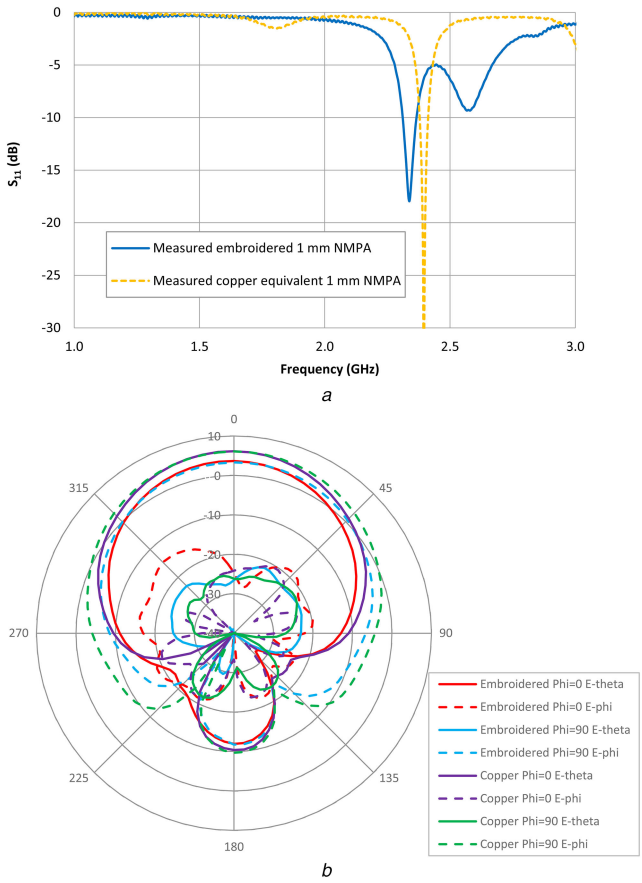


Fig. 8 Measured results of embroidered 1 mm NMPA on a Taconic RF45 substrate, compared with a etched copper 1 mm NMPA on the same substrate

(a) Measured S_{11} results, (b) Measured total gain patterns (in dBi)

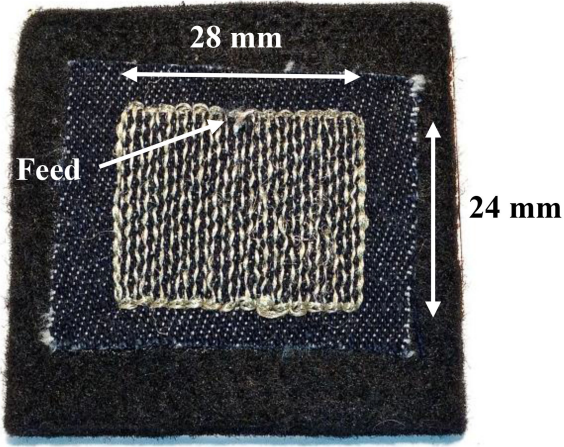


Fig. 9 Embroidered NMPA on flexible felt substrate

Nora-Dell was affixed on the felt by the thermal adhesive web. For the purpose of testing, a semi-rigid coaxial cable (RG405) was used as the feeding with the inner pin punched through the felt to make contact with the Amberstrand thread. The connection between the coaxial cable with the conductive textiles (Amberstrand and Nora-Dell) was reinforced by a drop of conductive epoxy. Other connections such as transmission lines or U.FL connectors can be used for low profile feeding, but they were not carried out in this work. Since etching a feed pad on the felt was not possible, the embroidered NMPA was placed face-up. The thermal melt adhesive web was used to affix the embroidered NMPA on the felt. The felt thickness was slightly decreased after thermal pressure. The total thickness of the substrate consisting of felt and adhered denim was approximately 4.3 mm. The multi-layer

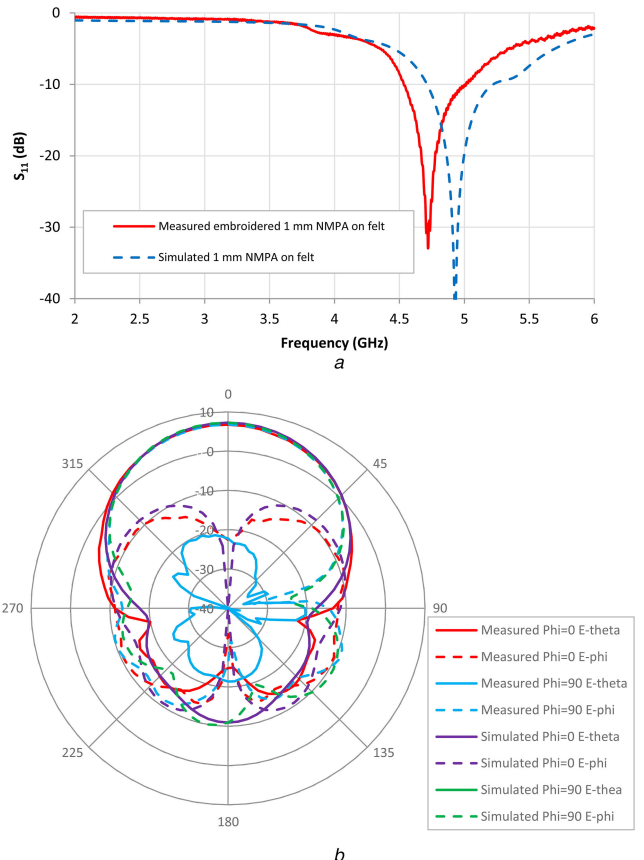


Fig. 10 Antenna performance of 1 mm NMPA on felt substrate

(a) Measured S_{11} results, (b) Measured antenna gain patterns (in dBi), compared with the simulation

substrate had approximately $\epsilon_r = 1.30$ and $\tan\delta = 0.008$ measured using SPDR. Since the smaller value of the permittivity of the substrate would increase the size of the patch antenna, in this section a smaller size embroidered NMPA was designed to work at 5 GHz wearable wireless local area networks (WLAN) frequencies. Furthermore, the skin depth decreased at higher frequencies, and therefore the metallisation thickness of the conducting thread became thicker than the skin depth. This meant the thin conducting layers of the embroidered thread could better support the currents and as a result lead to higher antenna efficiency.

The exterior dimensions of the NMPA were 28 mm \times 24 mm with 1 mm mesh spacing, which resulted in approximately 20% conductor coverage area. The optimal feeding location was obtained in simulations and it was on the middle of top horizontal current path – see Fig. 9. The measured S_{11} results are shown in Fig. 10a. As etching an NMPA on felt was not practical, a simulated result of a copper equivalent NMPA is included for comparison. In the simulation, the textile substrate was modelled as a 4.3 mm thick solid block with $\epsilon_r = 1.30$ and $\tan\delta = 0.008$ based on the SPDR measurement results. The meshes were modelled using low conductivity metal that was equivalent to the Amberstrand Silver 66 thread resistance. It can be seen that the resonant frequency of the embroidered NMPA is 205 MHz lower than the simulated result. This indicated that the actual electrical length of the embroidered patch was longer than the exterior dimension which agrees with the results in Section 4. Despite the frequency shift, the -10 dB bandwidth of the embroidered NMPA still covers the 5 GHz frequency point. The radiation patterns are shown in Fig. 10b. The embroidered NMPA has 6.8 dBi gain that includes the mismatch loss, compared with the simulated realised gain of 7.2 dBi. Measurement indicated that the embroidered NMPA realised 60% total efficiency with 20% conductor coverage.

6 Conclusions

This paper has presented the use of embroidered NMPAs that maintain good antenna gain and efficiency for significantly reduced specialised conducting threads usage, leading to lower cost and increased flexibility of the embroidered patch antennas. The NMPAs have similar current and electric field distribution as a solid patch antenna at the TM_{01} mode. Furthermore, the comparison between NMPAs and MPAs indicates that it is highly recommended to embroider textile-based patch antennas with the non-uniform mesh structures to maintain high antenna gain with reduced thread usage. It is worth noting that the actual length of the embroidered stitches is longer than the exterior dimensions of the embroidered patch. Therefore, the resonant frequency of an embroidered antenna is lower than the copper equivalent due to the extended electrical length. This indicates that the exterior dimensions of NMPA can be reduced relative to a solid patch antenna working at the same frequency.

The results have shown that fully textile embroidered 5 GHz NMPA had 60% antenna efficiency with only 20% of the conductor coverage. This is a highly satisfying outcome in terms of cost, flexibility and antenna performance. This will benefit potential wearable antenna applications since the cost of manufacturing and materials can be reduced. However, meshing the ground plane causes decreased front-to-back ratio radiation. Since the wearable antenna is placed close to human body, a solid ground plane offers better insulation between antennas and human body to prevent degraded antenna performance.

7 Acknowledgment

This work was funded by the Engineering and Physical Science Research Council through the Innovative electronics Manufacturing Research Centre.

8 References

- [1] Klemm, M., Troester, G.: 'Textile UWB antennas for wireless body area networks', *IEEE Trans. Antennas Propag.*, 2006, **54**, (11), pp. 3192–3197
- [2] Elliot, P.G., Rosario, E.N., Rama Rao, B., et al.: 'E-textile microstrip patch antennas for GPS'. IEEE/ION Position Location and Navigation Symp. (PLANS), 2012, pp. 66–73
- [3] Paradiso, R., Loriga, G., Taccini, N.: 'A wearable health care system based on knitted integrated sensors', *IEEE Trans. Inf. Technol. Biomed.*, *Publ. IEEE Eng. Med. Biol. Soc.*, 2005, **9**, (3), pp. 337–344
- [4] Pantelopoulos, A., Bourbakis, N.G.: 'A survey on wearable sensor-based systems for health monitoring and prognosis', *IEEE Trans. Syst. Man Cybern. C (Appl. Rev.)*, 2010, **40**, (1), pp. 1–12
- [5] Zhang, S., Chauraya, A., Whittow, W., et al.: 'Embroidered wearable antennas using conductive threads with different stitch spacings'. Antennas & Propagation Conf. (LAPC), Loughborough, 2012, pp. 1–4
- [6] Volakis, J.L., Zhang, L., Wang, Z., et al.: 'Embroidered flexible RF electronics'. IEEE Int. Workshop on Antenna Technology (IWAT), 2012, pp. 8–11
- [7] Kim, Y., Lee, K., Kim, Y., et al.: 'Wearable UHF RFID tag antenna design using flexible electro-thread and textile'. IEEE Antennas and Propagation Int. Symp., 2007, pp. 5487–5490
- [8] Zhang, S., Seager, R., Chauraya, A., et al.: 'Textile manufacturing techniques in RF devices'. 2014 Antennas and Propagation Conf. (LAPC), Loughborough, 2014, pp. 182–186
- [9] 'AmberStrand® fiber'. Available at: <http://www.metalcladfibers.com/amberstrand-fiber/>, accessed 12 December 2013
- [10] Zhang, S., Chauraya, A., Whittow, W., et al.: 'Repeatability of embroidered patch antennas'. Antennas & Propagation Conf. (LAPC), Loughborough, 2013, November, pp. 140–144
- [11] Seager, R., Zhang, S., Chauraya, A., et al.: 'Effect of the fabrication parameters on the performance of embroidered antennas', *IET Microw. Antennas Propag.*, 2013, **7**, (14), pp. 1174–1181
- [12] Karlsson, K., Carlsson, J.: 'Wideband characterization of fabrics for textile antennas'. 2012 6th European Conf. on Antennas and Propagation (EUCAP), 2012, pp. 1358–1361
- [13] Ivsic, B., Bonefacic, D., Bartolic, J.: 'Considerations on embroidered textile antennas for wearable applications', *IEEE Antennas Wirel. Propag. Lett.*, 2013, **12**, pp. 1708–1711
- [14] Ivsic, B., Bonefacic, D.: 'Implementation of conductive yarn into wearable textile antennas'. 2014 24th Int. Conf. Radioelektronika, 2014, pp. 1–4
- [15] Ito, K., Wu, M.: 'See-through microstrip antennas constructed on a transparent substrate'. Seventh Int. Conf. on (IEE) Antennas and Propagation, ICAP 91, 1991, vol. **1**, pp. 133–136
- [16] Turpin, T.W., Bakur, R.: 'Meshed patch antennas integrated on solar cells', *IEEE Antennas Wirel. Propag. Lett.*, 2009, **8**, pp. 693–696
- [17] Hautcoeur, J., Talbi, L., Hettak, K.: 'Feasibility study of optically transparent CPW-fed monopole antenna at 60-GHz ISM bands', *IEEE Trans. Antennas Propag.*, 2013, **61**, (4), pp. 1651–1657
- [18] Saberin, J.R., Furse, C.: 'Challenges with optically transparent patch antennas', *IEEE Antennas Propag. Mag.*, 2012, **54**, (3), pp. 10–16
- [19] Ahn, S., Choo, H.: 'A systematic design method of on-glass antennas using mesh-grid structures', *IEEE Trans. Veh. Technol.*, 2010, **59**, (7), pp. 3286–3293
- [20] Clasen, G., Langley, R.: 'Meshed patch antennas', *IEEE Trans. Antennas Propag.*, 2004, **52**, (6), pp. 1412–1416
- [21] Yasin, T., Bakur, R.: 'Circularly polarized meshed patch antenna using coplanar Y-shaped coupling feed', *Microw. Opt. Technol. Lett.*, 2014, **56**, (2), pp. 487–489
- [22] Chang, T., Lan, C., Kiang, J.: 'Mesh antennas with reduced size'. IEEE Antennas and Propagation Society Symp., 2004, vol. **4**, pp. 3832–3835
- [23] He, X., Gong, S., Ji, Y., et al.: 'Meshed microstrip patch antennas with low RCS', *Microw. Opt. Technol. Lett.*, 2005, **46**, (2), pp. 117–120
- [24] 'MCL-T whole-body solid SAM phantom'. Available at: www.mcluk.org/solidbodies.php, accessed 22 December 2015
- [25] 'Nora Dell'. Available at: <http://www.shieldextrading.net/pdfs/NoraDellCR.pdf>, accessed 12 September 2016
- [26] LessEMF: 'Pure Copper Polyester Taffeta Fabric'. Available at: <http://www.lessemf.com/fabric.html#1212>, accessed 20 March 2013
- [27] Krupka, J.: 'Measurements of the complex permittivity of microwave circuit board substrates using split dielectric resonator and reentrant cavity techniques'. Seventh Int. Conf. on Dielectric Materials, Measurements and Applications, 1996, pp. 21–24